

BOOSTING X-RAY OUTPUT WITH A GAS-PUFF BASED PLASMA OPENING SWITCH

A Thesis

Presented to the Faculty of the Graduate School
of Cornell University

in Partial Fulfillment of the Requirements for the Degree of
M.S.

by

Joseph Tucker Engelbrecht

August 2016

© 2016 Joseph Tucker Engelbrecht

ALL RIGHTS RESERVED

ABSTRACT

This thesis explores an idea for employing a low density gas-puff implosion as a plasma opening switch to rapidly transfer a current pulse into a more inductive load. A gas-puff on axial wire configuration is used to investigate the promise of this opening switch as a means of increasing the x-ray yield from the wire. We demonstrate the development of this configuration into a tunable current switch, and present promising x-ray measurements which suggest that this switch merits further investigation into its potential usefulness in x-ray source applications.

BIOGRAPHICAL SKETCH

Joseph Tucker Engelbrecht was born July 12, 1991 in the frigid reaches of Plattsburgh, a remote city just south of the parallel separating the peaceful state of New York from the tyrannical province of Quebec to the north. It was in this beautiful but impoverished region that Joey grew into a gentleman and a scholar; he was educated at Northeastern Clinton, a tiny border school kept in constant fear by the looming threat of northern aggression. He traveled south for collegiate study in the lowlands, earning his B.A. in Physics at Ithaca College in the spring of 2013. Joey chose to remain in the perceived safety of Ithaca to pursue graduate study in Applied Physics at Cornell University in the fall of 2013.

To Bowie, you freaky old bastard you.

ACKNOWLEDGEMENTS

This project has its origins in conversations between Profs. David Hammer and Bruce Kusse and Dr. John Giuliani from the Naval Research Lab. The idea was to enhance the x-ray yield from a standard cylindrical implosion by switching the current to a single-wire on axis just before the pinch. Initially a cylindrical wire array z-pinch was proposed, but experiments at Cornell had transitioned away from wire array loads in favor of gas-puff z-pinch implosions, so the experiment was designed around using the outermost gas-puff nozzle to inject a shell of gas which would carry the current pulse through the first phase of the shot. It was proposed that the radiation pulse produced at stagnation of the implosion could be enhanced if just before stagnation, the current could be switched from the imploding gas-puff plasma to an axial metal wire. It was argued that this current transfer could come about as a result of the growth of Magneto Rayleigh Taylor (MRT) instabilities interrupting current flow in the gas-puff plasma. A fast current switch from the initially lower inductance gas-puff plasma to the higher inductance axial wire should result in a higher dI/dt , offering the potential to produce a more intense x-ray burst, and more K-shell radiation than a gas-puff implosion or single wire explosion. The proposed experimental setup was similar to early gas-puff experiments performed at Cornell by Dr. Niansheng Qi, which employed a wire on axis to carry the foot of the current pulse, until the voltage was high enough to allow the gas to break down and carry current in a more typical gas-puff z-pinch implosion. The essential difference between the two experiments would be the use of an electron discharge preionizer, fired just before COBRA, which would ensure that the gas could carry current immediately and preserve the wire to take current at a later phase of the implosion.

I owe thanks to Drs. John Giuliani and Nicholas Quart from NRL for their contributions in establishing the idea behind this project, and also to Nick for coming up to Cornell to be a part of some of the experimental work. I have to thank Bruce not only for his guidance in the lab and in writing this thesis, but also for his roles outside the lab as a generous, if reluctant host, and as a drinking buddy who shared my enthusiasm for good food and whiskey. Dave deserves thanks for his important contributions to this thesis and to my graduate research career as a whole, as well as for serving as a formidable tennis opponent, although his red pen will haunt my dreams as a more fearsome stroke than his forehand. Qi was of course an indispensable resource, both when he was in Ithaca doing everything he could to help carry out these experiments, and for his wise counsel on all things gas-puff when he could not be present. I must also thank Dr. Phillip William Legeyt de Grouchy, for his help in turning me into a (semi-)competent researcher and gas-puff valve operator while he endured two miserable years on the wrong side of the pond. Thanks also to Dr. Tania Shelkovenko for taking the time to assist me, inform me, and otherwise attempt to convince me that x-ray spectroscopy was nothing to be intimidated by. I owe everyone else in the lab thanks, too, for contributing to this project in some way, large or small, technicians and students alike, with the exception of Levon, who was no help at all, despite his reportedly infinite patience. And my final acknowledgment must go to the espresso machine for the countless hours it spent in dutiful service while helping me prolong the writing of this document.

And I suppose my friends, family, and loved ones deserve some credit too. I love you guys!

LIST OF TABLES

2.1	X-ray detector readings for argon implosions onto a 50 μm Cu wire on axis, as a function of plenum pressure. Intensities are scaled to detector bias voltages. *Bolometer measurements were not obtained for the marked shots, so measurements taken on other shots with an identical load configuration and similar current pulses were used. Readings from 3799 and 3801 were used in place of 3942 and 3943, respectively.	19
2.2	Puff-on-wire shots for 50 μm Cu wire on axis. Si-diode intensities are arbitrarily scaled to 10 μm Cu filtered diode amplitude for Shot 3801	27

LIST OF FIGURES

1.1	Illustration of the basic principle behind plasma opening switches. Pre-injected plasma conducts current initially, then is opened by some mechanism, diverting the rest of the current pulse through a parallel load [1].	2
1.2	Diagram of double nozzle gas-puff valve. The experiments presented used only the outer nozzle, which has an outer diameter of 7 cm.	4
1.3	Photo of gas-puff nozzles, with wire hung from steel mesh over anode pins. Early experimental runs used this mesh to hold the wire, while later runs employed a hollow steel tube which was supported by two of the anode pins. Wire is affixed to brass cathode plug inserted into central nozzle.	5
1.4	Time lapse sketch of the experiment, with darker shades of red indicating later times of plasma evolution and current flow. The outer nozzle injects gas which carries the current initially, driving material in towards the wire on axis. Instabilities grow on the imploding shell, which it's believed could cause the current path to become pinched off or otherwise disrupted, forcing current to switch into the axial wire.	6
2.1	Shot 3640 - 2.0 psi Ar backing pressure, 100 μm Aluminum wire on axis. High mass shell gives a slow, stable run-in. Central wire carries no current, and can be seen to block emission from the back of the higher temperature gas-puff shell.	9
2.2	Shot 3646 - 1.0 psi Ar backing pressure, 100 μm Al wire on axis. Lower backing pressure produces faster implosion, increasing instability growth. Wire lights up in XUV before gas-puff column reaches axis.	11
2.3	Shot 3647 - 0.8 psi Ar backing pressure, 100 μm Al wire on axis. Lower backing pressure speeds up and further destabilizes the implosion, with wire emission beginning at an earlier stage. . . .	12
2.4	Shot 3747 - 0.6 psi Ar backing pressure, 50 μm Au wire on axis. This is a low density puff with a thin gold wire, which heats and breaks down quickly. The first two frames show hotspots on wire, shown in the next figure. The wire plasma has expanded significantly by the final frame.	12
2.5	Thomson scattering spectrum for Shot 3809 - 0.8 psi Ar backing pressure, 100 μm Cu wire on axis. Scattering signal apparent on 6 fibers with 1 mm separation, giving shell thickness measurement of 6 mm.	13

2.6	Shot 3747 - 0.6 psi Ar backing pressure, 50 μm Au wire on axis. Zoomed-in view of hotspots seen in the previous figure. Image taken at 110 ns into the pulse.	15
2.7	Shot 3807 - 0.8 psi Ar backing pressure, 25 μm Cu wire on axis. The thin copper wire heats quickly, allowing easier diagnosis of current flow as the wire expands and kinks.	15
2.8	Shot 3801 - 0.8 psi Ar backing pressure, 50 μm Cu wire on axis. The Rogowski coil trace dips sharply near 170 ns as indicated by the orange band, pointing to a change in inductance as current is forced to travel through the wire rather than the gas-puff plasma. The PCD picks up x-ray burst as the wire breaks down approximately 30 ns after the observed current switch.	16
2.9	Sensitivity of diamond PCD's versus energy. Low energy photons were blocked with plastic or metal filters. Filter responses are shown in Figure 2.11.	18
2.10	Sensitivity of silicon diode versus energy. Low energy photons were blocked with thick metal filters. Filter responses are shown in Figure 2.11.	18
2.11	X-ray transmission data from CXRO for for filters used in Table 2.1.	19
2.12	Comparison of Si-diode signals and PCD traces for several argon backing pressures, all with a 50 μm Cu wire on axis. All three argon shots used the filter set listed in Table 2.1. The no gas shot shown used thinner 10 μm Cu and 12 μm Ti filters on the diodes, so the signal intensities cannot be compared equivalently between this shot and the others.	21
2.13	Multiframe visible emission image of Shot 3802 - 0.8 psi Ar backing pressure, 50 μm Cu wire on axis. Oscilloscope traces shown for current pulse and PCD signal suggest that the x-ray burst coincides with the observed time of the gas-puff pinch.	24
2.14	Comparison between two intermediate pressure 0.6 psi Ar shots with a 50 μm Cu wire on axis. Shot 3950 produced a typical long pulse, and an intense x-ray burst during positive dI/dt . Shot 3948 inadvertently produced a short pulse, with x-ray burst coming after peak current, strongly suppressing x-ray burst, despite identical load conditions to Shot 3950.	26
2.15	XUV image series for mass-matched gas species comparison, which displays different time evolution of the current flow, particularly in krypton, despite the same gas mass in each shot. . . .	29
2.16	Si-diode signals comparison for Shot 3797 - Control shot with 50 μm Cu wire on axis, and Shot 3803 - 0.4 psi Kr backing pressure, 50 μm Cu wire on axis.	30
2.17	Shot 3961 - 0.35 psi Kr backing pressure, 50 μm Cu wire on axis.	32

2.18	Comparison of unfiltered x-ray pinhole images for two control shots and a puff-on-wire shot. Shot 3812 - 0.8 psi argon. Shot 3966 - 0.6 psi Ar on polypropylene fiber bundle. Shot 3967 - 0.6 psi Ar on 50 μm Cu wire.	34
2.19	Comparison of x-ray spectra for Shot 3751 - 0.8 psi Ar and Shot 3752 - 0.8 psi Ar on 50 μm Au wire. X-ray spectra taken using Mica crystal, with reflection order noted by Roman numerals. R and I represent resonance and intercombination lines, respectively. Argon only shot displays He like Ar satellites not seen in puff-on-wire shot, which displays only Au lines, supporting the conclusion that radiation from the wire is responsible for the bulk of the x-rays measured in puff-on-wire shots of 0.8 psi plenum pressure and lower.	35
2.20	Comparison of x-ray pinhole images for a single wire control shot, and similarly massed krypton and argon shots. From left to right, pinhole filters are 10 μm Cu, 12 μm Be, and 100 μm Be. .	37

CHAPTER 1

INTRODUCTION

1.1 Experimental Outline and Goals

Plasma opening switches have been thoroughly investigated in pulsed power experiments as a means for shortening the rise-time and increasing the peak power of a current pulse driven through a load since the 1970's [9]. The basic operating principle is illustrated in Figure 1.1. A pre-injected plasma, in parallel with another load, initially conducts a current pulse. At some point during the pulse, a disruption to the plasma "opens" this path, diverting the remainder of the pulse into the parallel load, on a timescale shorter than the rise-time of the generator. This rapid switching of the current path can also be accompanied by a similarly fast change in inductance, and therefore produce a sharp rise in the voltage at the load, by $V = Li + I\dot{L}$. This allows a plasma opening switch to increase the peak power able to be delivered to a suitable load by a pulsed-power generator, as it essentially serves as an additional stage of pulse compression before the load [7]. The usefulness of such a switch is immediately apparent, as it increases the capabilities of a generator without requiring mechanical upgrades, additional stored energy, or a new machine altogether.

The experiments described in this thesis were aimed at investigating a novel configuration involving a gas-puff valve, which seeks to take advantage of the potential power gain offered by a gas-puff z-pinch acting as a plasma opening switch to increase the peak power and yield of an x-ray source. The experiment is designed around the use of the outer nozzle of a double annular gas-puff valve to inject gas into the electrode gap of the COBRA 1 MA pulsed-power gen-

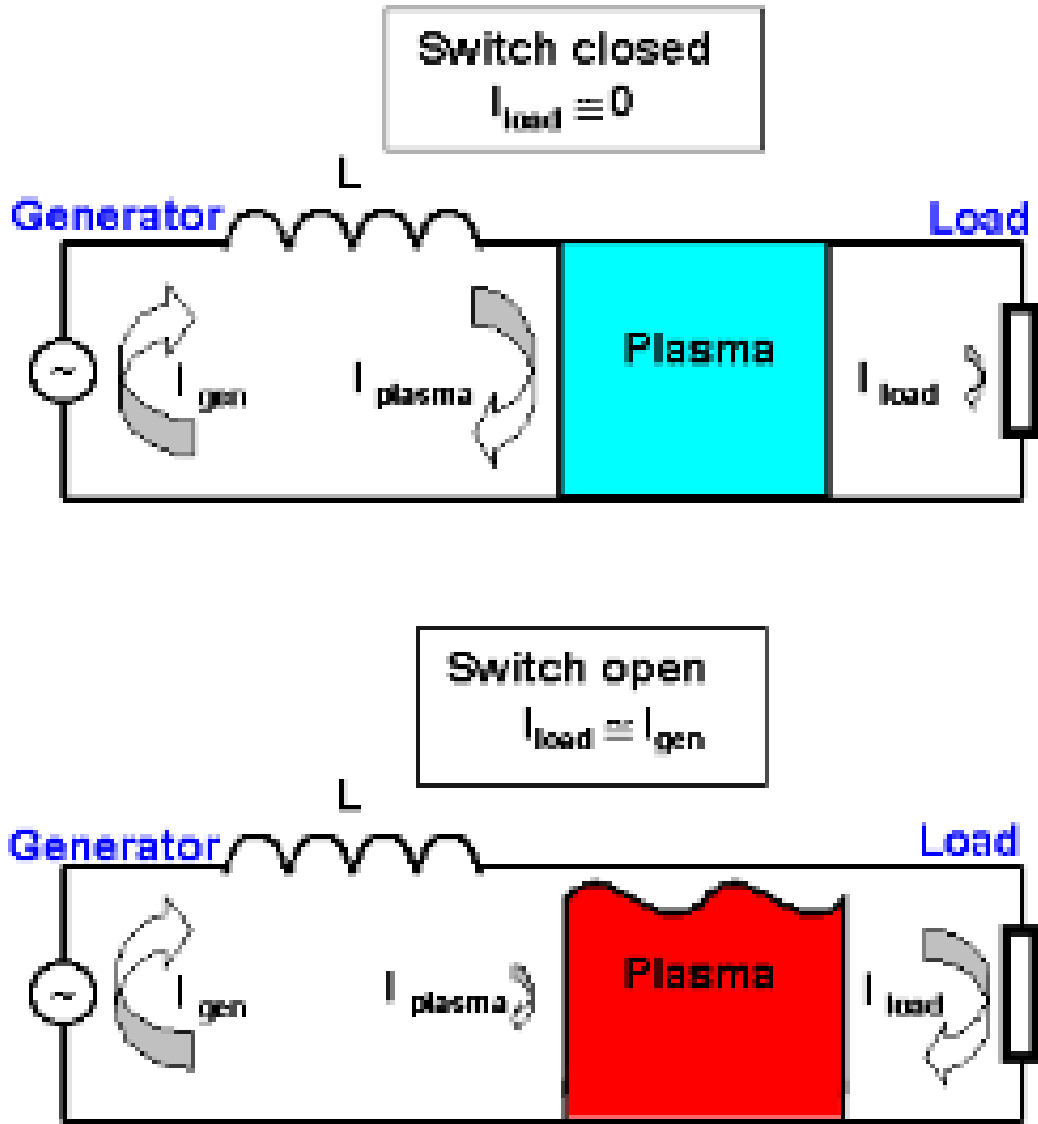


Figure 1.1: Illustration of the basic principle behind plasma opening switches. Pre-injected plasma conducts current initially, then is opened by some mechanism, diverting the rest of the current pulse through a parallel load [1].

erator. This gas is pre-ionized, and serves as the plasma which initially carries the current pulse, as shown in the illustration. Gas-puffs can be very efficient at x-ray production in their own right, but produce very little radiation above 3 keV, even when driven by much higher power generators [6], and so for applications which demand a harder spectrum, metal wire loads are preferred. In our experiment, a wire is affixed along the z-axis at the center of the gas-puff nozzle, and serves as the secondary, higher inductance load in parallel with the gas-puff plasma. This configuration is detailed further in the following section, but the basic intention is to induce the current to switch from the lower inductance gas-puff plasma into the higher inductance axial wire. If the switch opens at or near the peak of the current pulse, the fast power rise in the wire could increase the peak x-ray yield compared to a wire-only load, and produce a harder energy spectrum than a standard gas-puff z-pinch configuration, due to K-shell radiation from energetic electrons. If effective, this gas-puff switch could conceivably be paired with other types of central loads, such as a hybrid x-pinch, further increasing its effectiveness as an x-ray source for some applications.

The initial experiments with this puff-on-wire configuration were designed to test its functionality as an opening switch. These experiments demonstrated that current can be switched from the gas-puff plasma into the wire, and that the timing of the switch can be controlled by the gas-puff plenum backing pressure. After this was established, later experiments were targetted at investigating this configuration's possible utility as an x-ray source. Si-diode and PCD measurements of x-ray yields suggest that, given the right parameters, higher intensity x-ray signals could be achieved with the puff-on-wire shots than with a stand-alone wire or gas-puff. Our results detail the operational limits of the observed current switching behavior, and the criteria found to maximize x-ray produc-

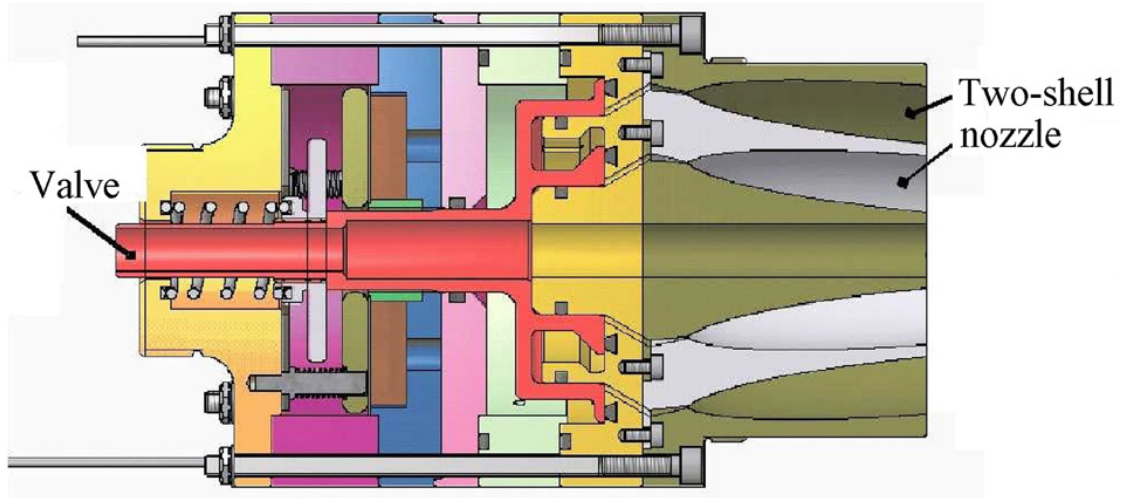


Figure 1.2: Diagram of double nozzle gas-puff valve. The experiments presented used only the outer nozzle, which has an outer diameter of 7 cm.

tion.

1.2 Experimental Setup

The majority of the data presented was taken using the double annular gas-puff valve shown in Figure 1.2. Some shots were also done using a triple nozzle valve, which shares the same construction as the double nozzle valve, with the exception of a different piston which enables the production of a central gas jet. The experiments presented in this thesis used only the outer nozzle of these valves, for which the two configurations are functionally identical, and so no distinction needs to be drawn between the two when comparing the results.

A wire was mounted along the z-axis at the center of the COBRA chamber between the gas-puff nozzle cathode and a ring of eight radially concentric steel

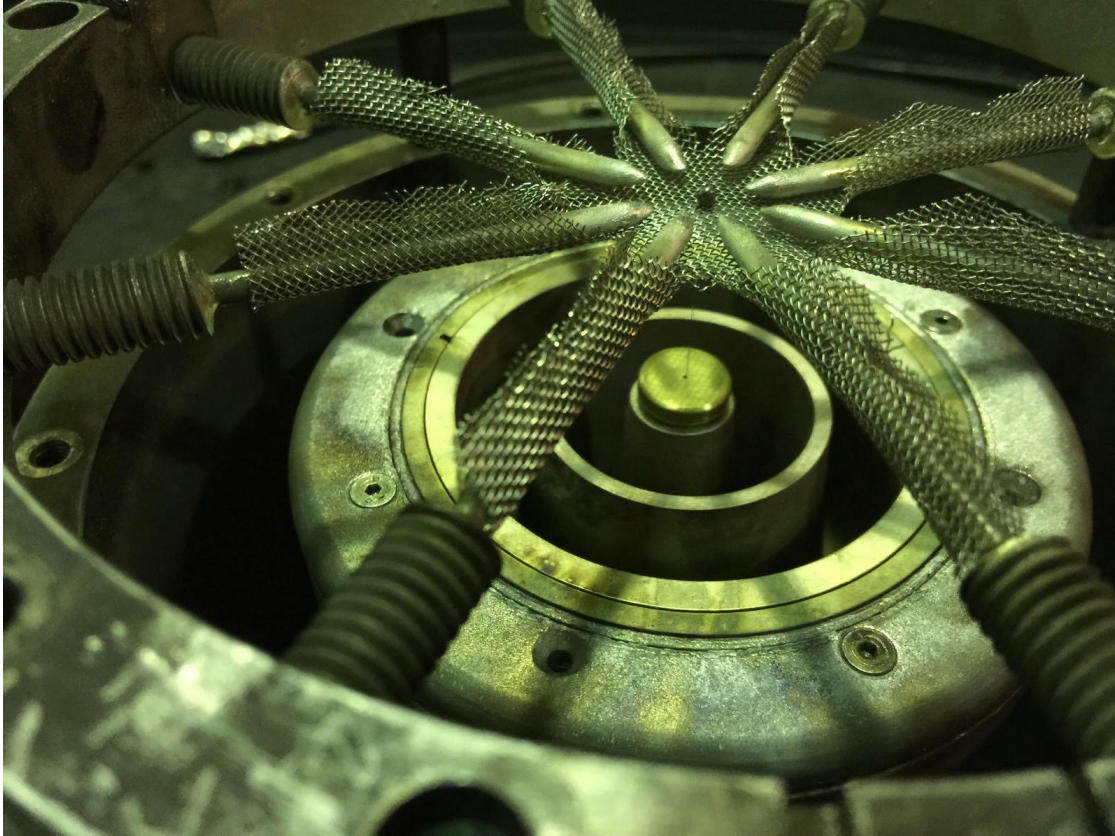


Figure 1.3: Photo of gas-puff nozzles, with wire hung from steel mesh over anode pins. Early experimental runs used this mesh to hold the wire, while later runs employed a hollow steel tube which was supported by two of the anode pins. Wire is affixed to brass cathode plug inserted into central nozzle.

pins at the anode. The wire is affixed to a brass plug which is inserted into the central nozzle of the gas-puff valve, shown in Figure 1.3. Over the course of the experiments, two different configurations were used to attach the wire to the anode. Early experiments were done using a steel mesh which wrapped around the anode pins, as shown in the photograph in Figure 1.3 in the picture, with the wire fed through one of the gaps in the mesh and held in place using a lead weight. Later experiments replaced the mesh with a hollow steel tube which was held in place by two of the anode pins, with a hole drilled to allow the wire

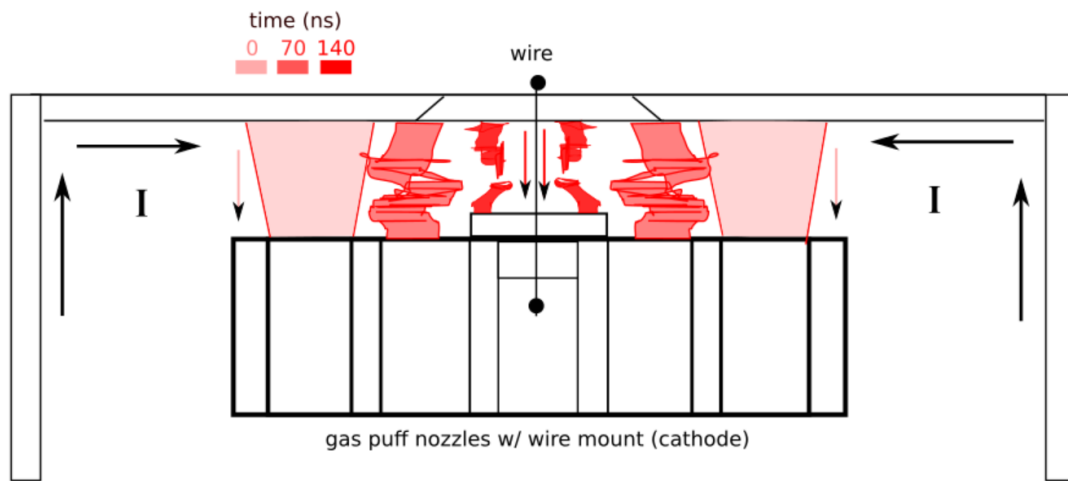


Figure 1.4: Time lapse sketch of the experiment, with darker shades of red indicating later times of plasma evolution and current flow. The outer nozzle injects gas which carries the current initially, driving material in towards the wire on axis. Instabilities grow on the imploding shell, which it's believed could cause the current path to become pinched off or otherwise disrupted, forcing current to switch into the axial wire.

to fastened through at the center. These two configurations showed no evidence of qualitative differences between the evolution of the plasma dynamics, and so we compare images interchangeably between both. However it is possible that electrode effects play some role in the x-ray production in this experiment, so all of the x-ray yield comparisons presented in Section 2.2 are performed using the second anode configuration with the hollow tube.

Figure 1.4 illustrates how our experimental configuration could function as a plasma opening switch. The gas injected by the gas-puff valve is preionized before COBRA's current pulse arrives. When the current pulse comes in, it flows initially through this plasma, rather than the wire, as it is a much lower inductance path. The current in the plasma is then compressed by its own magnetic

field, and driven radially inwards by the $J \times B$ force. It is well documented that Magneto Rayleigh-Taylor (MRT) instabilities develop as this implosion runs in towards the axis, and this instability growth is compounded by the lack of stabilizing inner mass provided by the inner nozzle puff [5]. Our hypothesis was that for gas-puff plasmas below some critical density, the current path through the unstable gas-puff plasma shell could open up due to the MRT growth, forcing current to find a new path to ground. This would result in a rapid switch of current into the axial wire. If this switch could be tuned to occur at or near the peak of the current pulse, the fast current rise could drive a faster breakdown of the wire at a higher peak power, thereby potentially increasing the peak power and yield of the x-ray burst produced as this wire explodes.

These experiments employed an array of diagnostics which we present in detail in Section 2. Extreme ultraviolet self emission cameras and a multi-frame optical camera were critical in tracking the evolution of the gas-puff implosion and current flow. Numerous photon detectors such as PCDs, silicon diodes, and a bolometer were used in measuring the radiation output, and x-ray pinhole cameras and an x-ray crystal spectrometer were used to further investigate the source of the high energy photons being produced. Laser interferometry and Thomson scattering measurements were used to infer variations in density and shell thickness.

CHAPTER 2
EXPERIMENTAL FINDINGS

2.1 Diagnosis of Current Switching with XUV Emission Imaging

The initial experimental goal was to verify our hypothesis that current would preferentially travel through the gas injected by the outer nozzle early in the current pulse, and not through the central wire. To test this, initial shots using the puff-on-wire configuration were done with a high outer plenum backing pressure, which produces a correspondingly high mass gas-puff, slowing down and stabilizing the implosion against instability growth. Extreme ultraviolet (XUV) pinhole images taken by two 4-frame time integrated XUV self-emission cameras, with 10 ns MCP gate lengths, were used to characterize these implosions. Large 200 μm pinholes were used, offering the highest signal intensity at the expense of resolution. All of the shots presented in this section are for argon outer nozzle-only gas-puffs, with a wire on axis.

Figure 2.1 shows a four frame sequence of XUV images for a 2.0 psi argon outer shell backing pressure with a 100 μm wire on axis. The 2.0 psi Ar backing pressure is much higher than used in typical mass-profiled implosions on COBRA, which employ an outer:inner:center argon backing pressure of 1:3:8 psi, with the 1 psi injected by the outer nozzle accounting for 70% of the mass [2]. This high shell mass results in a slow run-in of material, which still has not reached the axis well after the peak of the current pulse, as is clearly shown in Figure 2.1. Throughout this sequence of images the axial wire can be seen at

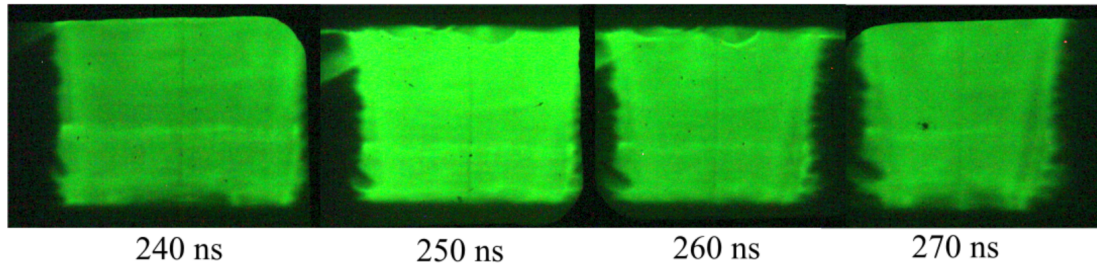


Figure 2.1: **Shot 3640** - 2.0 psi Ar backing pressure, 100 μm Aluminum wire on axis. High mass shell gives a slow, stable run-in. Central wire carries no current, and can be seen to block emission from the back of the higher temperature gas-puff shell.

the center as a dark vertical band shadowing the emission from the back of the gas-puff shell, indicating that the wire is not hot enough to radiate in the XUV even late in time after the peak of the current pulse. The fact that the lower temperature wire is visible blocking the emission from the back of the shell indicates that it is not carrying current, and also implies that the gas-puff plasma is optically thin in the XUV, even in this high density case. This high-mass implosion accelerates slowly, and therefore has a low MRT instability growth rate in comparison to lower mass implosions presented in later figures, with only mild instability growth on the trailing edge of the gas-puff plasma. Given the slow instability growth of the implosion there is no mechanism for the current flow in the gas-puff plasma to be cut off and forced through the wire. The XUV images confirm our expectation that in the case of a high mass gas-puff implosion, current is carried entirely by the imploding gas-puff plasma, and not in the central wire.

With the behavior of the load in this relatively stable case established, we then sought to investigate whether we could cause current to switch from the gas-puff plasma into the wire. Obviously in the case that the plenum backing

pressure is set to 0, all of the current pulse travels through the wire, as it has no other path, and we get a single wire explosion. The question is if there is an intermediate backing pressure at which the current starts out in the gas but is forced into the wire as its path is pinched off or depleted by the unstable dynamics of the gas-puff implosion. To investigate this we began lowering the outer nozzle plenum pressure, thereby increasing the acceleration of the gas-puff implosion and the growth rate of instabilities that form on this shell.

Keeping the 100 μm Aluminum wire at the center, and stepping down the outer plenum backing pressure in increments of 0.2 psi, we observed the same behavior seen in Figure 2.1, with no evidence of current in the wire despite seeing a measurably faster run-in and instability growth in each case, until we reached backing pressures of 1.2 psi and lower. At this pressure we began observing different behavior in the XUV images. The wire could initially be seen to block emission from the back of the hotter gas-puff shell, but then would light up brightly in later frames, indicating that it has been heated to the point that it is a brighter source of XUV emission than the surrounding gas-puff plasma. This behavior is illustrated clearly in the 1.0 psi argon shot in Figure 2.2, which shows a transition from the wire silhouetting the gas-puff column to emitting more brightly than it over the course of 20 ns.

While the XUV images show that below the observed pressure threshold of 1.2 psi we are able to observe the wire being heated, they do not necessarily indicate that the wire has begun carrying a significant portion of the current. Other possible heating mechanisms include the collision of the leading edge of the imploding shell with the wire on axis, or radiative heating by emission from the imploding gas-puff column. However there is no reason that radiative

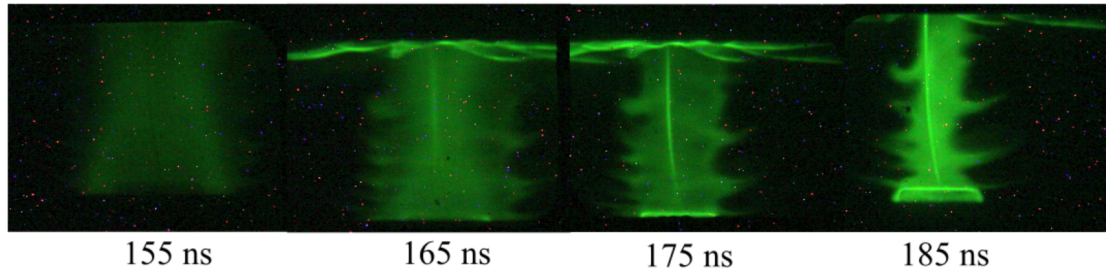


Figure 2.2: **Shot 3646** - 1.0 psi Ar backing pressure, 100 μm Al wire on axis. Lower backing pressure produces faster implosion, increasing instability growth. Wire lights up in XUV before gas-puff column reaches axis.

heating should be correlated with the plenum pressure. If anything, the higher mass shots offer a longer time over which the wire can be heated by radiation, yet even at late times these shots exhibit a cold wire blocking thermal emission from hotter gas-puff plasma. The possibility remains that in higher backing pressure shots, the onset of radiation occurs when gas-puff plasma begins colliding with the wire. However as backing pressure is reduced further to 0.8 and then 0.6 psi, as shown in Figs. 2.3 and 2.4, the wire can be observed lighting up in the XUV progressively earlier in time, with the outer edge of the imploding shell visible at correspondingly larger radii. If the illumination of the wire were being caused by an impact of material, this would indicate that the shell thickness is increasing dramatically as plenum backing pressure is lowered, which is not consistent with our interferometry or Thomson scattering measurements.

The shell thickness of a typical 1:3:8 argon gas puff implosion on COBRA has been independently measured by laser interferometry and Thomson scattering to be approximately 5 mm [8]. A raw Thomson scattering spectrum for a 0.8 psi argon on wire shot is presented in Figure 2.5, and gives a shell thickness estimate of 6 mm. This could indicate that the shell is marginally thicker in lower

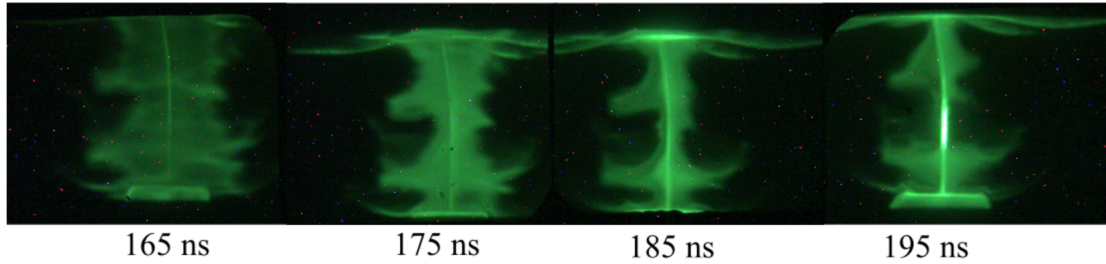


Figure 2.3: **Shot 3647** - 0.8 psi Ar backing pressure, 100 μm Al wire on axis. Lower backing pressure speeds up and further destabilizes the implosion, with wire emission beginning at an earlier stage.

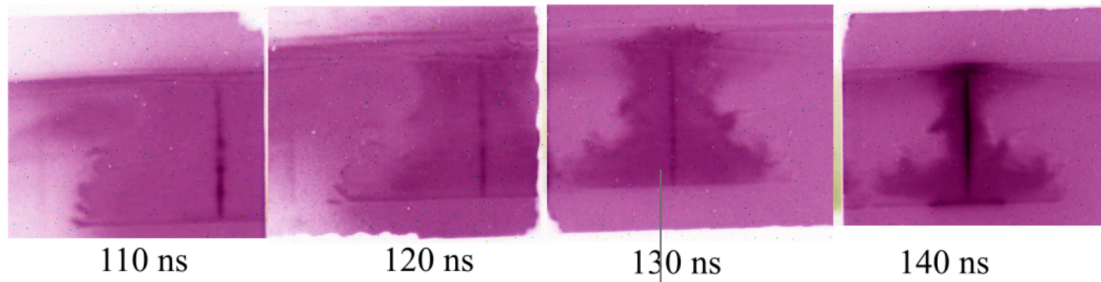


Figure 2.4: **Shot 3747** - 0.6 psi Ar backing pressure, 50 μm Au wire on axis. This is a low density puff with a thin gold wire, which heats and breaks down quickly. The first two frames show hotspots on wire, shown in the next figure. The wire plasma has expanded significantly by the final frame.

backing pressure shots without the presence of a stabilizing inner puff, but does not deviate significantly from typical measurements. Importantly there is no scattering signal close to the axis, with the outer edge of the shell approximately 10 mm away from reaching the wire, indicating that at this stage there is likely no significant amount of material colliding with the wire ahead of the pinch.

As a scale reference, the cathode plug holding the wire, which is visible at the bottom of the XUV images, measures 16 mm in diameter. In Figure 2.2, we see that the wire is first fully radiating in the third frame, where the trailing edge

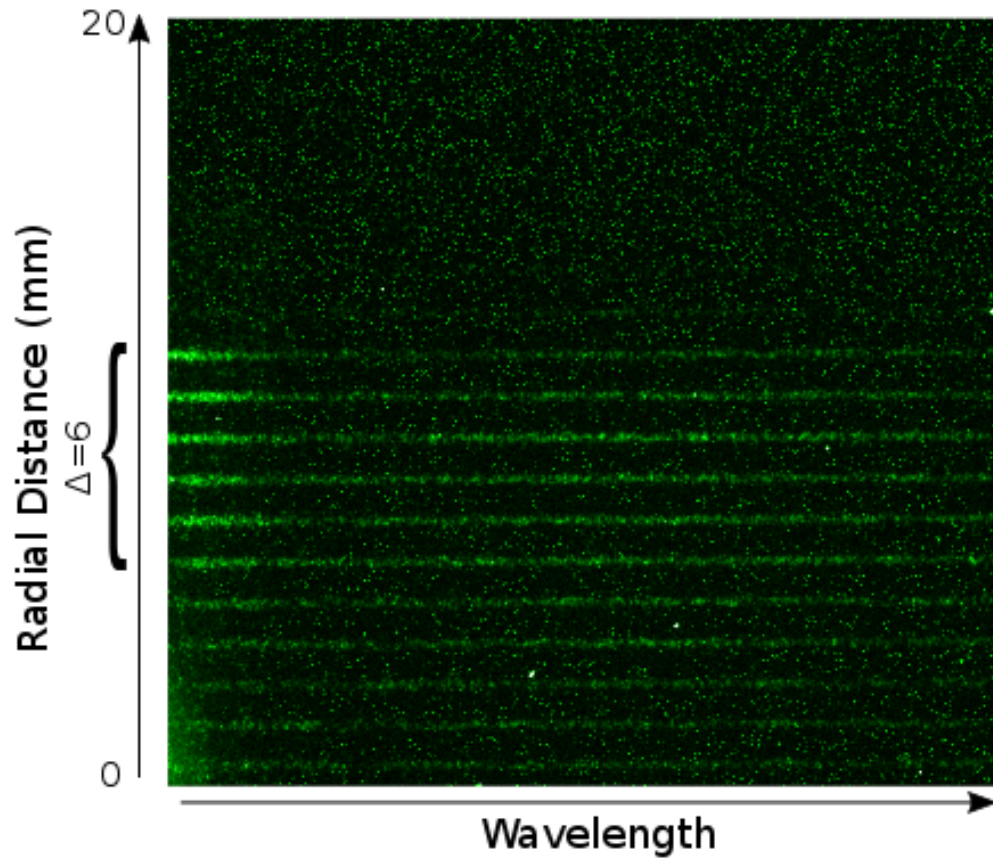


Figure 2.5: Thomson scattering spectrum for **Shot 3809** - 0.8 psi Ar backing pressure, 100 μm Cu wire on axis. Scattering signal apparent on 6 fibers with 1 mm separation, giving shell thickness measurement of 6 mm.

of the shell is at approximately the radius of the edge of this plug. This suggests that the shell would need to be at least 8 mm thick to begin hitting the wire at this stage of the implosion. In Figure 2.3 the wire is already radiating in the first frame, at which point the shell radius is several millimeters larger in diameter than the cathode insert, and in Figure 2.4 the wire is emitting brightly even earlier, when the outer edge of shell is at least 12 millimeters from the central axis.

Given our measurements and understanding of the implosion dynamics, the observed heating of the wire at these early times cannot be ascribed to collision of inflowing plasma.

This conclusion points to current flow as the probable explanation for the heating of the wire. Further evidence in support of this explanation can be seen in the first frame of Figure 2.4, which is blown up in Figure 2.6. It shows what look like hotspots caused by $m=0$ instabilities forming on the wire, a further indication of current flow. These hotspots are even more apparent in x-ray pin-hole images of the wire, presented in Section 2.3.2. By the final frame of Figure 2.4, the wire has expanded significantly beyond its initial radius, as seen in typical single-wire explosions. Other shots with plenum pressures of 0.8 psi or lower show evidence of instabilities developing on the wire, including Shot 3807 shown in Figure 2.7. The load configuration for this shot was 0.8 psi Ar backing pressure with a $25\ \mu\text{m}$ Cu wire at center. This thinner wire heats faster, allowing for easier diagnosis of the current transfer, with the image showing the wire expanding and what looks like a mild kink or $m=1$ instability forming on the wire just before the pinch.

Rogowski current monitor traces often show a rapid drop in dI/dt near the time that XUV cameras suggest current transfer taking place, as shown in Figure 2.8. These notches in the current trace are typical hallmarks of inductive current switching [3]. We take this evidence, in addition to what we see in the XUV images, as a demonstration of our ability to switch current from the gas-puff shell into the axial wire. In identifying this behavior as being evident of current switching, these XUV images further suggest that the timing of this switch is dependent upon the plenum backing pressure. Identifying the characteristic

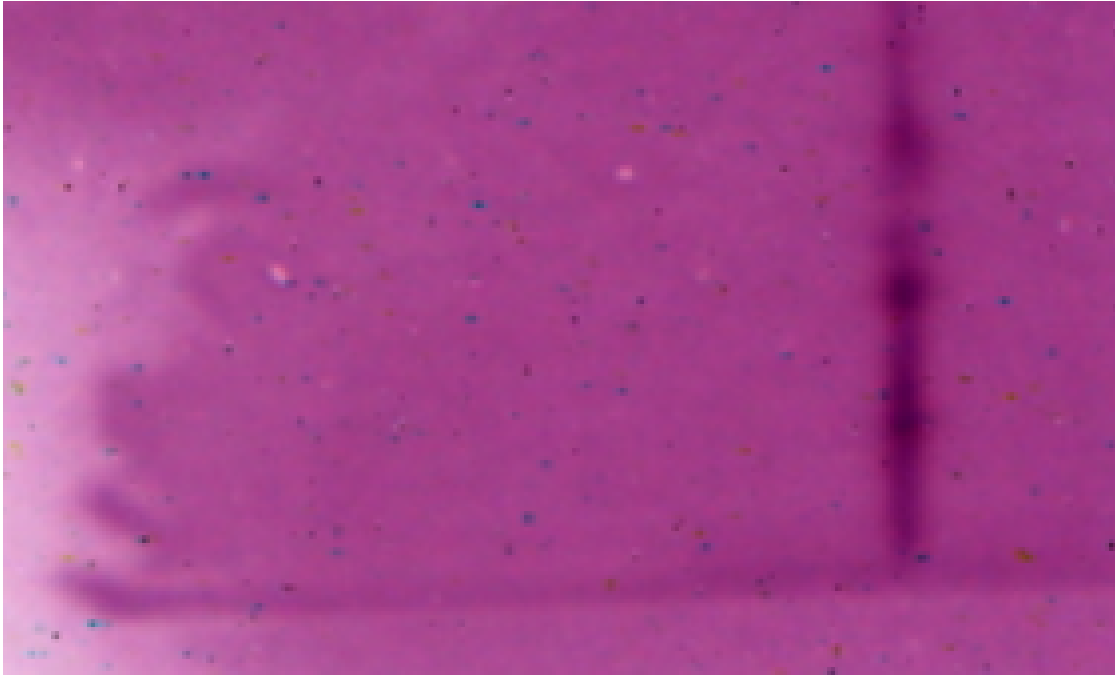


Figure 2.6: **Shot 3747** - 0.6 psi Ar backing pressure, 50 μm Au wire on axis. Zoomed-in view of hotspots seen in the previous figure. Image taken at 110 ns into the pulse.

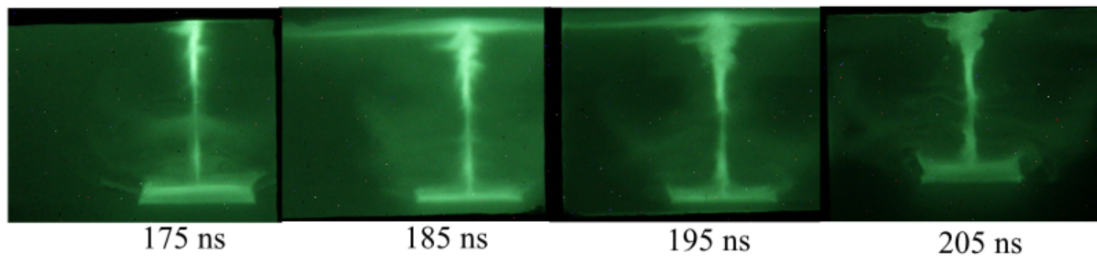


Figure 2.7: **Shot 3807** - 0.8 psi Ar backing pressure, 25 μm Cu wire on axis. The thin copper wire heats quickly, allowing easier diagnosis of current flow as the wire expands and kinks.

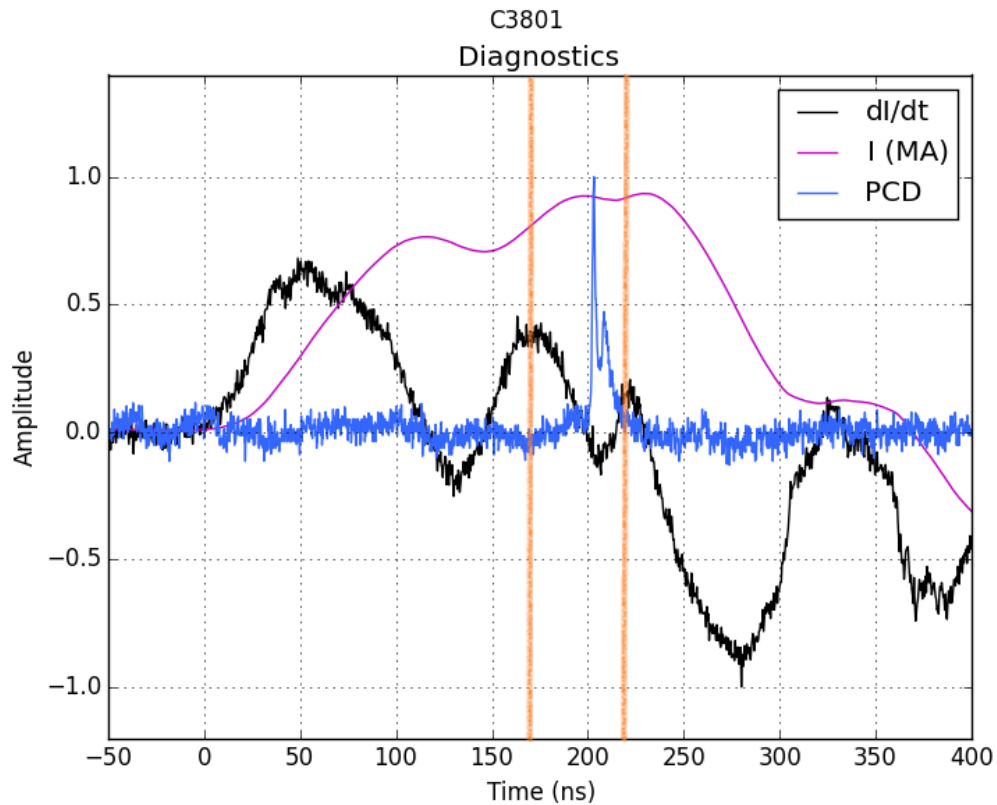


Figure 2.8: **Shot 3801** - 0.8 psi Ar backing pressure, $50\ \mu\text{m}$ Cu wire on axis. The Rogowski coil trace dips sharply near 170 ns as indicated by the orange band, pointing to a change in inductance as current is forced to travel through the wire rather than the gas-puff plasma. The PCD picks up x-ray burst as the wire breaks down approximately 30 ns after the observed current switch.

current notches allows us to pinpoint exactly when this fast current switch is taking place. Being able to exert this control over the switch timing is critical if this configuration is to be developed into a useful source.

2.2 X-ray Yield Measurements

Having established that current can be transferred from the gas-puff plasma into the axial wire, and that we are able to control the timing of this current switch with the plenum backing pressure, we began investigating the x-ray output of this configuration. Several diagnostics were used in profiling the x-ray production. Diamond photoconducting detectors, or PCDs, were used to measure the instantaneous soft x-ray output. These PCD's have a flat response up to about 5 keV, as seen in Figure 2.9. Harder x-rays up to 10 keV were detected by uncalibrated Si-diodes with thick metal filters. The energy response of these diodes can be seen in Figure 2.10. A nickel bolometer with a flat response up to 2 keV was used to make absolute measurements of the energy radiated in that spectral range [10].

2.2.1 Plenum Backing Pressure Dependence of X-ray Yield

Our first objective in investigating the radiative output of the puff-on-wire shots was to characterize how adjusting the plenum backing pressure affected the x-ray production, as this parameter controlled the timing of the current switch. Table 2.1 shows peak x-ray detector readings for a series of shots for which the central wire and gas species were kept constant, and only plenum backing pressure was varied, with an argon outer puff imploded onto a 50 μm Cu wire on axis.

This data set reveals a conspicuous trend in the total yield as the backing pressure is reduced. High backing pressure shots produce altogether less radi-

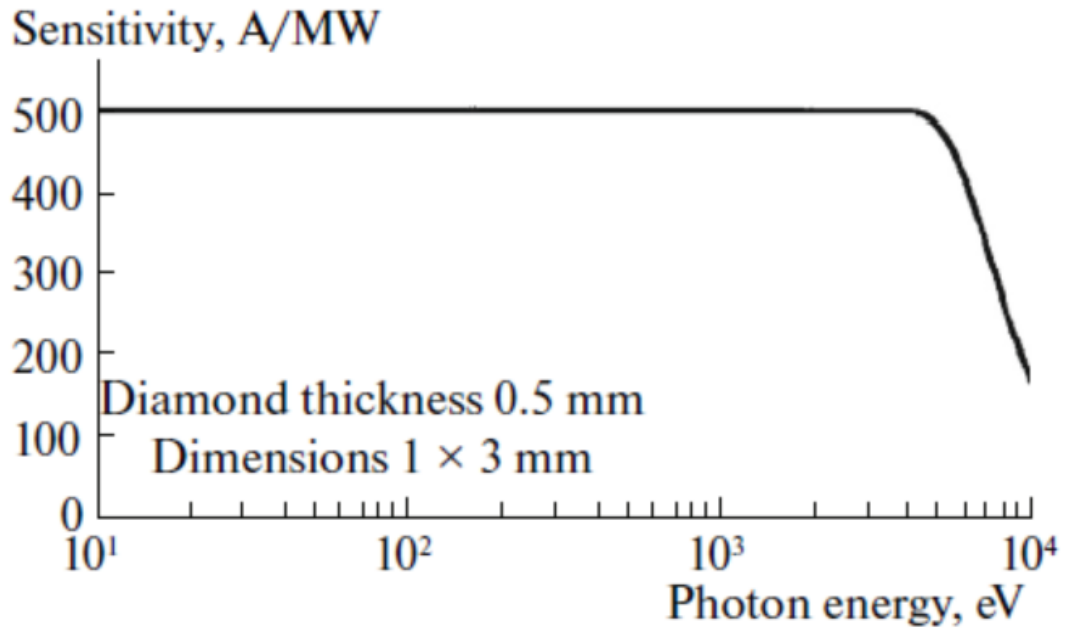


Figure 2.9: Sensitivity of diamond PCD's versus energy. Low energy photons were blocked with plastic or metal filters. Filter responses are shown in Figure 2.11.

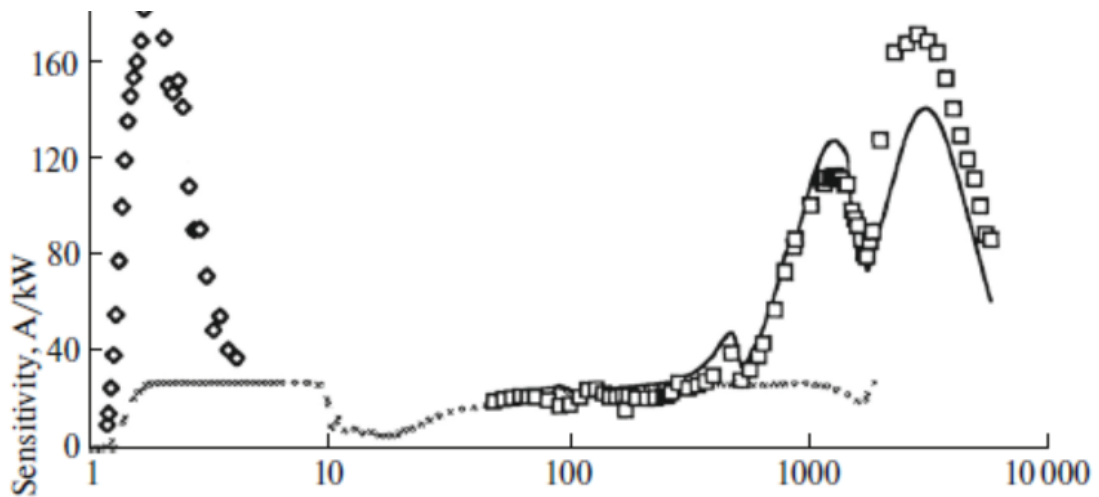


Figure 2.10: Sensitivity of silicon diode versus energy. Low energy photons were blocked with thick metal filters. Filter responses are shown in Figure 2.11.

X-ray Production for Decreasing argon Pressure						
Shot	Outer [psi]	Peak I (MA)	100 μm Al SiD (7+ keV)	30 μm Cu Si-D (7-9 keV)	6 μm Mylar PCD (1+ keV)	Bolo. (kJ)
3942	Ar [1.0]	0.914	.10	.07	.06	1.6*
3943	Ar [0.8]	1.069	.16	.12	.08	1.2*
3950	Ar [0.6]	0.874	.32	.20	.17	3.3
3954	Ar [0.5]	0.857	.76	.53	.45	3.3
3951	Ar [0.4]	0.749	.31	.20	.26	2.5
3952	Ar [0.2]	0.749	.25	.18	.11	3.7
3953	–	0.783	.88	.57	.63	4.1

Table 2.1: X-ray detector readings for argon implosions onto a 50 μm Cu wire on axis, as a function of plenum pressure. Intensities are scaled to detector bias voltages. *Bolometer measurements were not obtained for the marked shots, so measurements taken on other shots with an identical load configuration and similar current pulses were used. Readings from 3799 and 3801 were used in place of 3942 and 3943, respectively.

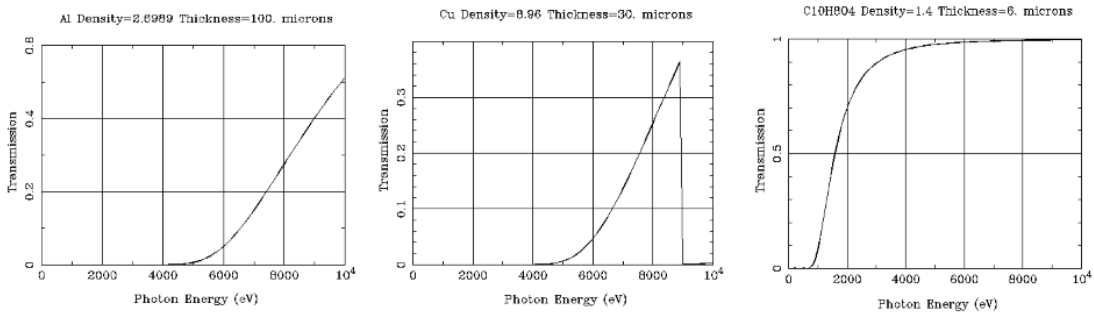


Figure 2.11: X-ray transmission data from CXRO for filters used in Table 2.1.

ation, with minimal readings on the Silicon diodes, PCDs and bolometer for 0.8 psi Ar pressure and above. These yields increase dramatically for intermediate pressures near 0.5 psi, and then drop again for lower pressure shots. While no argon shots produced peak x-ray bursts as strong as those measured in the single-wire control shot, interesting comparisons can be drawn between the highest yield 0.5 psi Ar shot and the wire-only control shot. The 100 μm Al filtered diode, which is picking up only photons above approximately 7 keV, as shown in the filter transmissions in Figure 2.11, gives a significantly higher peak signal in the control shot. However, the diode with the 30 μm Cu filter, which also transmits photons above 7 keV, but has a high energy cutoff due to the Cu K-edge at 9 keV, picks up very similar peak signals in the control shot and the 0.5 psi Ar-on-wire shot. The bolometer and PCD signals were also substantially lower for this 0.5 psi argon shot than the control, suggesting that it is just this narrow energy range which displays a similar output between the two shots. This could be an indication that there is more energy coming from line radiation in this range, particularly from the copper $K\alpha$ line at 8.05 keV. Unfortunately x-ray spectroscopy data was not collected for these shots, so we are as yet unable to confirm this possibility.

The x-ray signals show the same strong sensitivity to plenum backing pressure that's seen in the XUV images, and support our interpretation of the evolution of the current flow over the course of these shots. This may not be readily seen when comparing the peak x-ray signals presented in Table 2.1, but analysis of the temporal profiles of these x-ray signals for shots with a range of argon backing pressures, as shown in Figure 2.12, reveals more. Comparing these detector traces, there are obvious distinctions that can be drawn between shots, beyond just the overall magnitude of the x-ray burst, which reflect the changing

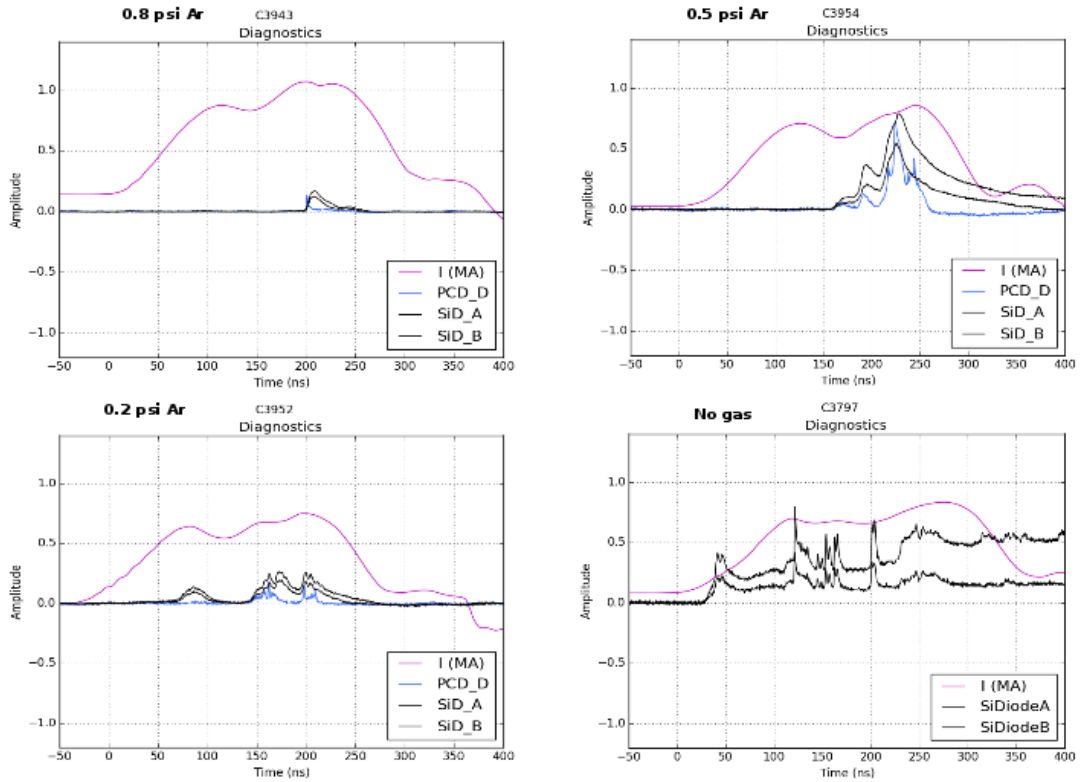


Figure 2.12: Comparison of Si-diode signals and PCD traces for several argon backing pressures, all with a $50 \mu\text{m}$ Cu wire on axis. All three argon shots used the filter set listed in Table 2.1. The no gas shot shown used thinner $10 \mu\text{m}$ Cu and $12 \mu\text{m}$ Ti filters on the diodes, so the signal intensities cannot be compared equivalently between this shot and the others.

dynamics of the current flow as a function of the argon backing pressure. The most striking effect is the progression from a single x-ray burst near the peak of the current pulse in the higher backing pressure shots, to a multitude of x-ray events occurring at earlier stages of the current pulse as the backing pressure is reduced. This behavior is consistent with the faster current transfer at lower backing pressures which was picked up in the XUV images.

2.2.2 Control Shots Without a Conducting Wire

One possible interpretation of these results is that the higher argon mass shots are more "gas-puff-like", and so exhibit a single x-ray burst as the implosion pinches and stagnates, whereas the lower mass argon shots can conversely be seen as more "single wire-like", with the wire carrying most of the current from an early time, consequently resulting in coronal plasma repeatedly re-pinching onto the expanding wire surface [4]. This simplification of the dynamics is appropriate, as it captures the sensitivity of the experiment to the gas backing pressure, and neatly divides the experiments into two regimes, with x-ray production optimized at their meeting point. However this simplification implies that in the higher gas pressure cases, it is the pinching gas-puff plasma which is responsible for the x-ray burst, rather than wire breakdown. In order to explore the latter possibility, control shots using similar argon pressures were performed with no wire at the center. These shots produced no hard x-ray emission, as measured by the Silicon diodes. The soft x-ray emission measured by the PCDs also decreased by an order of magnitude, likely because the shots were undermassed and lacked the stabilizing inner puff present in typical gas-puff implosions, and therefore did not produce a stable pinch.

These wire-less control shots do not rule out the possibility that the central wire serves as a target for the gas-puff plasma to pinch onto, which experiments have shown can strengthen the pinch and amplify the x-ray output in higher mass, more stable gas-puff implosions [11]. Indeed, at backing pressures of 0.8 psi and above, the x-ray burst seems to correlate closely with the observed time of the gas-puff pinch, as shown in Figure 2.13. Several additional experiments were performed to test if this was the case, by introducing central

mass which would not produce any significant x-rays on its own. These control experiments included a shot where the conducting wire was replaced with an insulating polypropylene fiber bundle, which wouldn't carry much current, but could provide a stabilizing target or centering agent for the pinch. The presence of central mass for these shots did increase the x-ray yield measurably, allowing the Silicon diodes to pick up small signals at the time of the pinch, and nearly doubling the soft x-ray emission measured by the PCDs. However none of the measured x-ray signals were on the order of those obtained for shots with a conducting wire present at similar argon pressures. Furthermore, for Ar pressures above 0.5 psi, the conducting wire shots displayed a clear trend of increasing hard x-ray production as the argon backing pressure was reduced. The control shots using other targets seemed to exhibit the opposite trend, with higher gas backing pressures yielding all around higher x-ray output. This makes sense, as even at a relatively high 0.8 psi outer plenum argon backing pressure, the gas-puff is injecting almost 50% less gas than would be used in a typical mass-profiled gas-puff shot that was optimized for x-ray production [2]. The differing response to changes in backing pressure, and the large increase in overall yield suggests that even in higher backing pressure cases, the presence of a conducting wire plays a greater role in the x-ray production than merely serving as a target for inflowing plasma. The source of this radiation is investigated further in Section 2.3.1, which examines x-ray pinhole images and spectra for puff-on-wire shots.

The fact that the conducting wire shots displayed the opposite correlation with outer plenum backing pressure that was seen using non current-carrying targets serves as further evidence that even the higher mass puff-on-wire shots are evolving differently than typical gas-puff implosions. Comparison of XUV

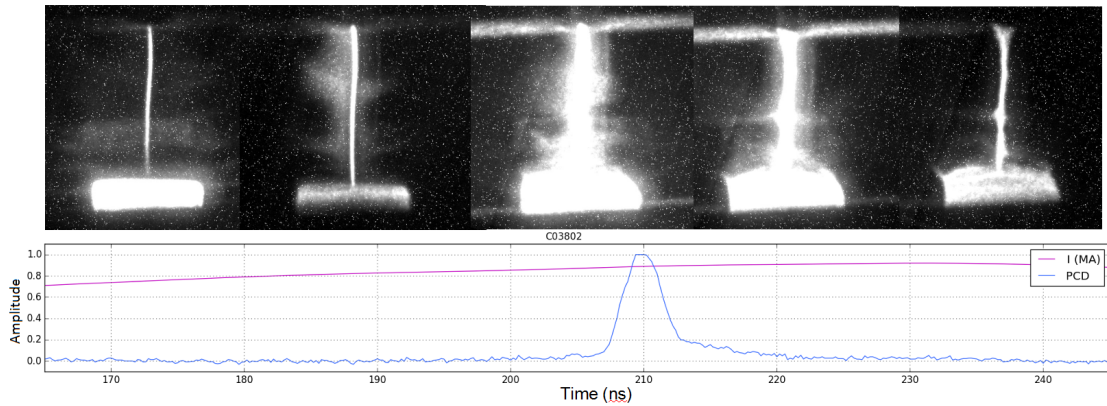


Figure 2.13: Multiframe visible emission image of **Shot 3802** - 0.8 psi Ar backing pressure, 50 μm Cu wire on axis. Oscilloscope traces shown for current pulse and PCD signal suggest that the x-ray burst coincides with the observed time of the gas-puff pinch.

images against the diode and PCD signals suggests the onset of x-ray production before the gas-puff plasma pinches onto the wire. This evidence points to breakdown of the wire due to late time current flow being responsible for the bulk of the measured x-ray bursts, rather than pinching gas-puff plasma. Several high mass shots also display dual x-ray bursts, with an initial hard x-ray burst followed up 20+ ns later by a softer burst, likely from the argon coming in and pinching on the already expanding wire.

2.2.3 Pulse-Shape and Voltage Dependence of X-ray Yield

Further examination of the detector signals presented in Figure 2.12 prompts the question of why the x-ray production is seemingly optimized at intermediate backing pressures near 0.5 psi. The answer seems to lie in the current pulse shape itself, and is heavily reliant on our use of COBRA's long pulse mode of operation, with a 200 ns rise time. At these intermediate pressures, the gas-

puff plasma seems to be able to carry the current throughout at least the first 150 ns, taking it through the reversal of dI/dt before switching into the wire, and so x-ray production is suppressed until just before the peak of the current pulse. Shots that meet this criterion, such as the 0.5 psi Ar shot shown in Figure 2.12, typically display a single, high intensity x-ray burst which is sustained for 30+ ns, and dies out quickly as dI/dt goes negative after the current peak. Higher argon pressures, such as the 0.8 psi case shown in the figure, hold off the x-ray burst until peak current, and evidently produce a temporally sharper but lower intensity burst of radiation. Likewise, at very low pressures current switches into the wire at earlier times, but the x-ray burst is suppressed as dI/dt reaches its first reversal, before the second part of the pulse comes in. As dI/dt turns positive again, a second distinct x-ray burst is produced, as the plasma re-pinches onto the expanding wire. This secondary burst is typically not as intense as those observed in intermediate pressure shots, where the initial wire breakdown occurs after this local minimum in the current pulse shape.

The x-ray measurements all point to dI/dt , and therefore voltage, at the time of wire breakdown being the single most critical factor in determining the yield of a given puff-on-wire shot. This is illustrated well by the comparison between two shots with differing pulse shapes, but identical load conditions shown in Figure 2.14. Both shots used 0.6 psi argon outer plenum backing pressure, with a 50 μm wire at center. This is near the optimum intermediate pressure that we've found maximizes x-ray production, and we see in the first plot of Shot 3950 that we get quite a strong x-ray burst, which begins just as dI/dt begins rising again. The adjacent plot is for Shot 3948, which had the same gas backing pressure, but had COBRA's two Marx generators fire out much closer than intended, giving a short pulse. This faster current rise means that the current has already peaked

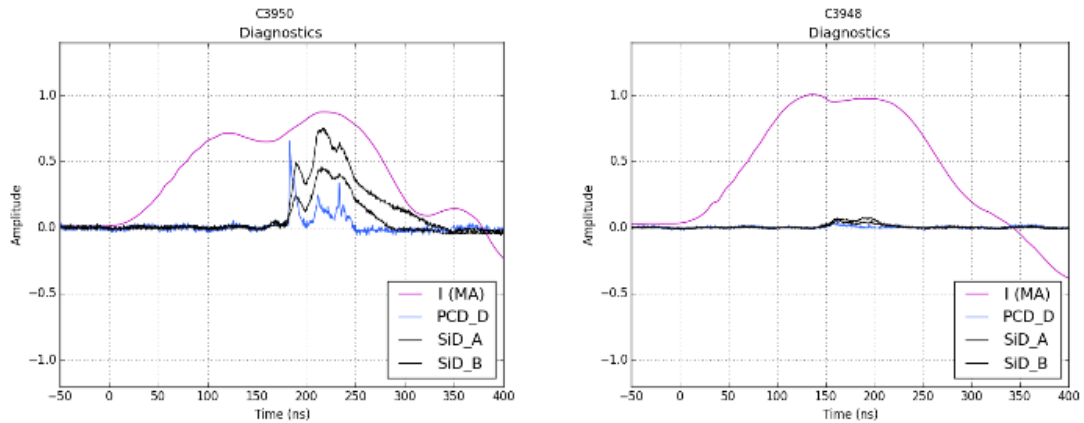


Figure 2.14: Comparison between two intermediate pressure 0.6 psi Ar shots with a 50 μm Cu wire on axis. Shot 3950 produced a typical long pulse, and an intense x-ray burst during positive dI/dt . Shot 3948 inadvertently produced a short pulse, with x-ray burst coming after peak current, strongly suppressing x-ray burst, despite identical load conditions to Shot 3950.

by the time the wire takes current and breaks down, which almost completely destroys the x-ray output, despite the fact that nearly 1 MA of current is flowing in the load at the time of the burst. We can conclude from this result that the ideal load parameters we've established for this configuration are limited to the long current pulse shape on COBRA and may not be generally applicable.

This finding also raises the possibility that the switch could be optimized for short pulse operation, if the backing pressure were reduced enough for it to open in 80 ns or less. For the sake of consistency, long pulses were used almost exclusively in these experiments, aside from the odd accidental short pulse. Because the gas-puff was pressurized for long pulses, these short pulse shots inevitably gave diminished x-ray yields. However the short pulse mode of operation offers a higher maximum dI/dt and peak power than can be achieved

Mass-matched Gas Species Comparison						
Shot	Outer [psi]	Peak I (MA)	10 μm Cu Si-diode	12.5 μm Ti Si-diode	15 μm Al PCD	Bolometer (J)
3801	argon [0.8]	0.934	1	0.82	1.56	1200
3803	krypton [0.4]	0.754	2.25	1.84	–	800
3805	neon [1.6]	0.927	0.62	0.68	0.67	1600

Table 2.2: Puff-on-wire shots for 50 μm Cu wire on axis. Si-diode intensities are arbitrarily scaled to 10 μm Cu filtered diode amplitude for Shot 3801

with a long pulse. If the plenum backing pressure were reduced to the point that current switched into the wire much earlier, the higher dI/dt just before peak current could amplify the effect and drive yields up further.

2.2.4 Mass-Matched Gas Species Comparison

Our experiments also explored the effect that varying gas-species would have on x-ray production, with neon and krypton being substituted for argon for several shots, the results of which are presented in Table 2.2. In order to compare shots with different species, an attempt was made to match the mass of the gas injected for each shot. An ideal gas at thermal equilibrium maintains a constant number density at a constant pressure, by $PV = Nk_B T$. Applying this to a neon puff, which has roughly half the atomic mass of argon, we see that the backing pressure needs to be doubled to produce a gas-puff implosion of similar mass. Likewise, krypton produces a similarly massed implosion with roughly half the backing pressure of argon.

This comparison of different gas species yielded an interesting result. All of the measurements seem to indicate that changing the gas species has a dramatic

impact on the x-ray production. This was unexpected, as our understanding up until this point had been that in these lower mass implosions, most of the x-ray output was originating from the breakdown of the wire, rather than in the gas-puff pinch. It was particularly surprising to see such large variation in the silicon diode signals, as previous shots had shown that without a wire present, the diodes did not pick up any signal at all. This seemed to show conclusively that all of the hard radiation being picked up on the Si-diodes was coming from the wire, and should be relatively unaffected by the gas species, assuming similar implosion dynamics. These measurements, in addition to others not shown in the table, suggest that hard x-ray production increases with the atomic mass number of the gas, or as the backing pressure is reduced.

Taken as a whole, these x-ray measurements, along with XUV images of these shots, suggest that the current switch, and subsequent wire breakdown and gas-puff pinch events, are unfolding differently between these shots. Figure 2.15 shows a sequence of XUV images for the shots presented in Table 2.2, and seems to show the implosion evolving in a distinctly different fashion between shots, particularly for the krypton shot, which exhibited the highest hard x-ray yields. For this shot the gas-puff plasma column is dim, with almost all of the radiation coming from the wire, which has already expanded significantly in the first frame, indicating that it has started taking current much earlier in the pulse than in the other two shots.

With the evidence against radiative differences between the gases being responsible for the difference in x-ray output, and given the intended mass-matching, the only significant parameter which is varied between this series of shots is the particle number density. Both the XUV images and the x-ray di-

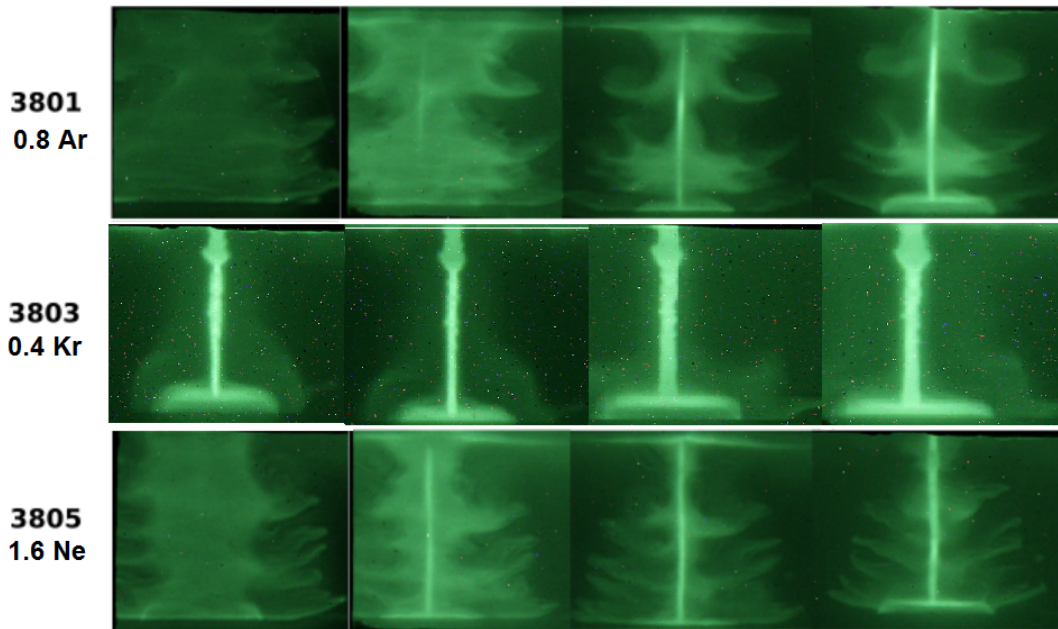


Figure 2.15: XUV image series for mass-matched gas species comparison, which displays different time evolution of the current flow, particularly in krypton, despite the same gas mass in each shot.

agnostics point to the lower pressure krypton shot behaving more like a single wire explosion, while for the higher pressure shots with the lighter gases, more energy goes into the gas-puff implosion. This is consistent with the bolometer measurements as well, which show higher radiative energy outputs for the higher pressure shots. Our measurements have shown that gas-puff implosions typically give a softer x-ray spectrum and show higher radiation conversion efficiency than single wire shots, with mass-profiled gas-puff implosions yielding upwards of 6 kJ of radiative output. Similar current pulses driven through a wire yield less than 1 kJ.

The observed differences in the dynamics as the implosion evolves could possibly be explained if the mechanism responsible for switching current into

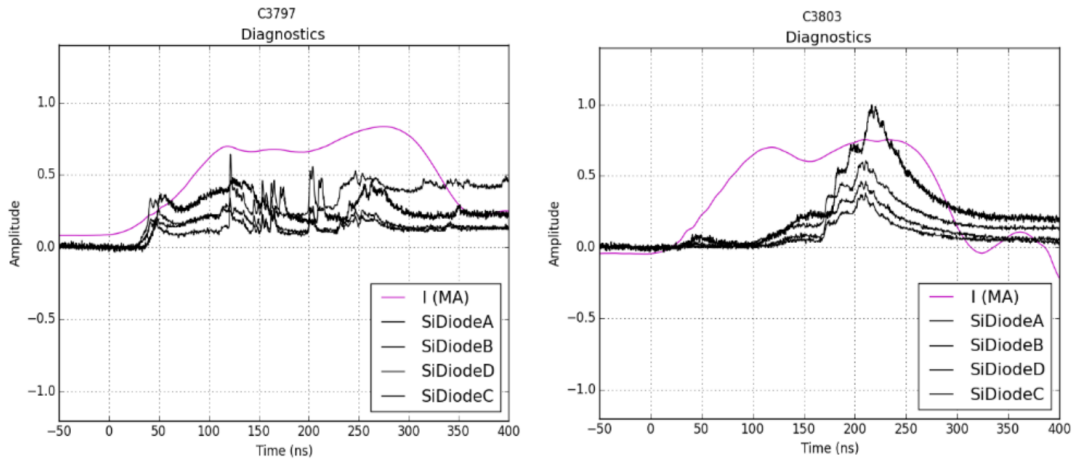


Figure 2.16: Si-diode signals comparison for **Shot 3797** - Control shot with $50\ \mu\text{m}$ Cu wire on axis, and **Shot 3803** - 0.4 psi Kr backing pressure, $50\ \mu\text{m}$ Cu wire on axis.

the axial wire is the depletion of charge carriers. This could happen earlier in the pulse for the low pressure krypton shot, due to the lower particle number, with the gas-puff plasma able to sustain current longer in the argon and neon cases, delaying the current switch. Theoretically this should mean that argon and neon could produce similarly high hard x-ray yields if used at a similar 0.4 psi pressure. Up until this point, only argon backing pressures above 0.6 psi had been investigated, but this result prompted us to explore lower pressures, and find the "sweet-spot" near 0.5 psi presented in Section 2.2.1.

Interestingly, Shot 3803, the krypton shot, produced significantly higher peak hard x-ray output than seen in a standard single-wire explosion, Shot 3797, something that had not been seen with argon. Si-diode yields for these two shots are shown in Figure 2.16. Three of the four Si-diodes showed higher intensities with the Kr-on-wire than seen in the single wire only shot, with the two filtered diodes that lack high energy cutoffs, the $15\ \mu\text{m}$ Al and the $25\ \mu\text{m}$

Be, picking up more than twice the intensity recorded in the wire only shot, indicating a significantly harder output spectrum. The diode response over the course of the pulse shows different behavior in the Kr-on-wire shot than in the wire-only shot, which begins x-ray production shortly after the foot of the current pulse comes in. In the krypton shot there is no significant x-ray output until dI/dt reverses and becomes positive again around 170 ns, at which time a sharp uptick is observed, and a sustained burst continues for at least the next 50 ns. This lack of early-time x-rays indicates that the current switch is behaving in a similar but accelerated manner to that seen in the higher backing pressure cases, with current flow initially in the gas-puff plasma, then transitioning into the wire, suppressing wire breakdown until current has nearly peaked. This shot conforms well to our prescription for an ideal puff-on-wire shot. However it is not certain if the increased yield seen in this shot is related to the switch to a heavier gas species, or if it is a case of perfectly matched load conditions for the current pulse.

Subsequent shots were performed at similar krypton backing pressures, in attempt to replicate and elucidate this result. This effort produced easily the highest yield shot seen over the course of the experiment, presented in Figure 2.17. This shot, which used a 0.35 psi krypton backing pressure, completely saturated both Si-diodes up to their bias voltage of 35 V, despite having 30 μm Cu and 100 μm Al filters. The PCD trace was cut-off by the range of the oscilloscope, but displays a negative response after the burst, which typically indicates detector saturation as well. Taking the copper filtered Si-diode voltage as a minimum, this shot produced at least 1.8 times the peak radiation in the 7-9 keV range as was measured in the highest yield single-wire only shot. This shot is further investigated with x-ray pinhole images in Section 2.3.2.

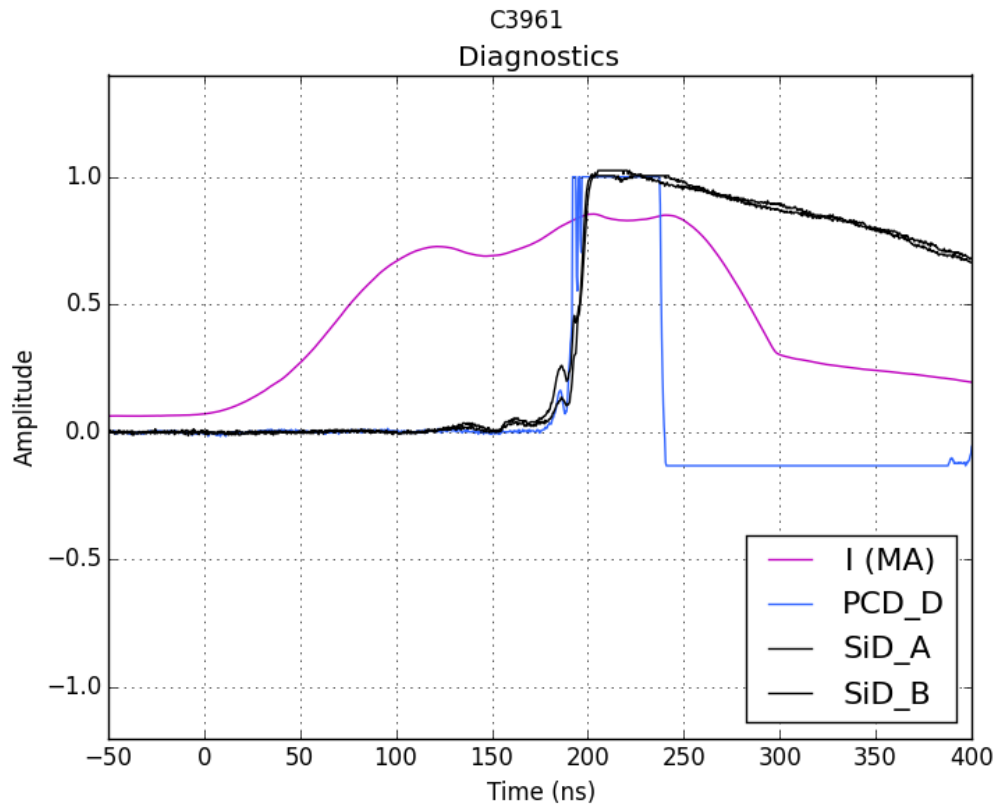


Figure 2.17: **Shot 3961** - 0.35 psi Kr backing pressure, 50 μm Cu wire on axis.

Measuring such a marked increase in the x-ray output for these krypton shots may indeed be indicative of a real effect, as argon was more thoroughly explored, but did not seem to produce x-ray bursts on the scale produced with krypton. However this was only the case for the two shots presented; six krypton shots were performed in the same backing pressure regime, with the remaining shots producing yields more in line with those seen using argon. Similarly, one shot with argon produced an unexpectedly high x-ray yield which was cut-off by the scale setting on the oscilloscopes. This outlier may well have produced x-ray outputs on a similar scale to the high yield krypton shots, but the peak signals went unmeasured. The sensitivity of the experiment to cur-

rent pulse shape and small changes in backing pressure made reproduction of these high yield shots difficult. Therefore although most of the results point to krypton as being more effective than argon for maximizing x-ray production, we can't definitively establish that this is more than just a consequence of ideally matched gas backing pressure and current pulse shape. Interestingly, the optimum pressure for krypton was found to be slightly lower, at 0.35 - 0.4 psi, as opposed to 0.5 psi with argon. These pressures do not correlate neatly with respect to either mass or ion number density, and so connections drawn between these parameters and the current switching mechanism remain inconclusive as well.

2.3 X-ray Pinhole Imaging and Spectroscopy

2.3.1 Isolating the X-ray Production Region and Source

For some shots, a phosphor image plate pinhole camera with several different x-ray filters was fielded, allowing us to identify the source region of the high energy x-rays picked up on the detectors. A comparison between several of the argon control shots and an argon on wire shot is presented in Figure 2.18. The first image shows a 0.8 psi argon implosion with no central wire. The low gas density coupled with the lack of stabilizing inner mass produces a highly unstable implosion, so the argon does not pinch well, and instead we see diffuse clouds of emission, with the most concentrated radiation coming from a single area near the anode at the top of the image. The middle image shows the 0.6 psi argon control shot using a polypropylene fiber bundle on axis, which provided

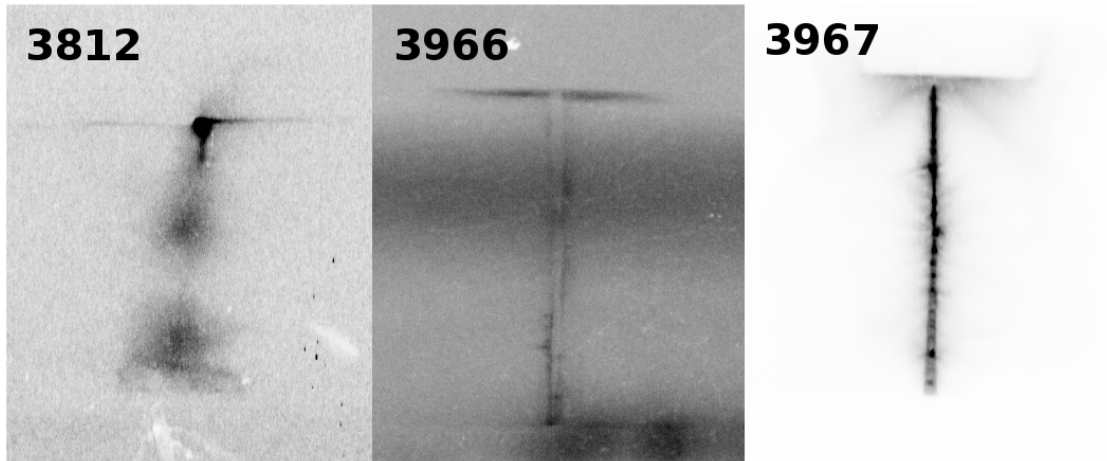


Figure 2.18: Comparison of unfiltered x-ray pinhole images for two control shots and a puff-on-wire shot. **Shot 3812** - 0.8 psi argon. **Shot 3966** - 0.6 psi Ar on polypropylene fiber bundle. **Shot 3967** - 0.6 psi Ar on 50 μm Cu wire.

a central target for the gas-puff plasma to pinch onto. This shot produced better x-ray yields than measured with no central mass, despite the low intensity seen in this image. A more uniform layer of emission is visible on the surface of the insulating fiber, indicating a more axially uniform pinch. The final image shows another 0.6 psi argon shot, this time with a 50 μm Cu wire on axis. This intermediate pressure is near the optimum that we've found to maximize x-ray production, and a dramatic increase in intensity is apparent in the image when viewed alongside the control shots. The emission is concentrated almost entirely in the location of the wire, rather than just where material is pinching on

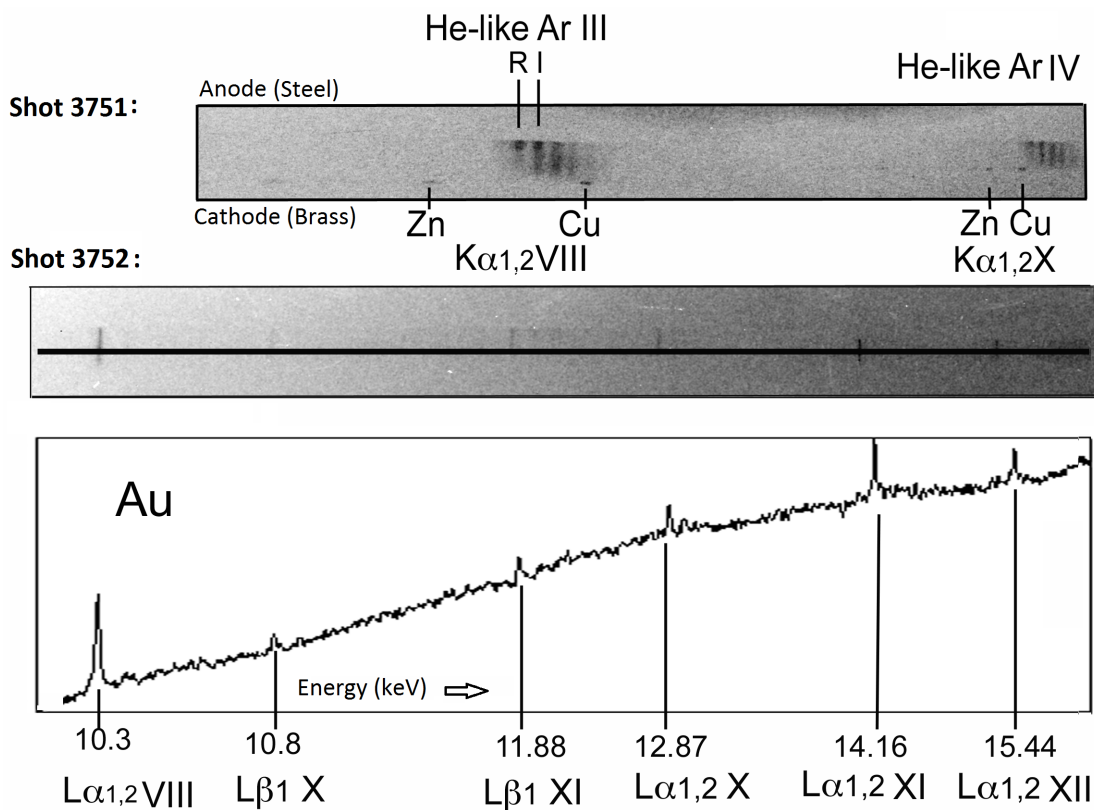


Figure 2.19: Comparison of x-ray spectra for **Shot 3751** - 0.8 psi Ar and **Shot 3752** - 0.8 psi Ar on 50 μm Au wire. X-ray spectra taken using Mica crystal, with reflection order noted by Roman numerals. R and I represent resonance and intercombination lines, respectively. Argon only shot displays He like Ar satellites not seen in puff-on-wire shot, which displays only Au lines, supporting the conclusion that radiation from the wire is responsible for the bulk of the x-rays measured in puff-on-wire shots of 0.8 psi plenum pressure and lower.

the surface, as in the previous image. The entire area of the wire is emitting, with several obvious hotspots visible along its length, a typical characteristic of single wire explosions. These pinhole images distinctly contrast with one another, and support our conclusion that the vast majority of the x-rays measured in these puff-on-wire shots originate from the copper wire itself, rather than pinching gas.

X-ray spectra were also gathered for early puff-on-wire shots, and proved useful in confirming the source of the x-ray production. While we were unable to field an x-ray spectrometer for any of the low gas pressure copper wire shots presented in the previous section, we were able to compare the x-ray spectra of Ar-on-wire shots to an Ar-only control without a wire present. Figure 2.19 presents two spectra taken using a mica crystal spectrometer; Shot 3751 was a 0.8 psi argon shot with no central wire, while Shot 3752 used the same argon pressure but had a 50 μm gold wire on axis. In the Ar-only shot, helium-like argon resonance, intercombination, and satellite lines are present, which do not show up at all in the shot with the wire present. The spectrum from the puff-on-wire shot exhibits primarily Au L-shell lines. The absence of any argon lines in the spectra of puff-on-wire shots confirms that even in higher backing pressure, "gas-puff like" puff-on-wire shots, it is the wire which is responsible for the measured x-rays, rather than pinching gas-puff plasma.

2.3.2 Krypton vs. Argon Pinhole Image Comparison

Figure 2.20 presents a set of x-ray pinhole images with several different filters, comparing krypton and argon puff-on-wire shots of similar masses to a single-wire explosion. Shot 3961, the krypton shot presented, yielded the highest measured x-ray signals of all shots, saturating all of the x-ray detectors. The x-ray pinhole images produced bear a close resemblance to the single wire control shot, with both showing a series of distinct x-ray hotspots along the entire length of the wire. Notably, the krypton shot picked up a more intense image through the copper filter than the control, perhaps another indication of stronger copper K-shell line radiation in the puff-on-wire shots than is seen in the single wire

3965 - 50 μm Cu Wire



3961 - 0.35 psi Kr on 50 μm Cu Wire



3967 - 0.6 psi Ar on 50 μm Cu Wire



Figure 2.20: Comparison of x-ray pinhole images for a single wire control shot, and similarly massed krypton and argon shots. From left to right, pinhole filters are 10 μm Cu, 12 μm Be, and 100 μm Be.

shots.

The bottom image was taken for an argon-on-wire shot, with a slightly lower mass density than the krypton shot above it, but close to the ideal 0.5 psi pressure found to produce the highest x-ray yields for argon. This shot produced a moderate x-ray output, and displayed good timing with respect to the current pulse, but detector signals were an order of magnitude lower than those

measured in the krypton shot above, which is reflected in the emission pattern seen on the image plate. Rather than displaying many individual hotspots, the wire is radiating uniformly along its length, with only a few hotspots apparent. The absence of these hotspots suggests that the current in the wire may not have been high enough to produce $m = 0$ instabilities, thus the coronal plasma can compress more symmetrically along the axis, limiting hotspot formation and reducing the overall output [4]. If this explanation is correct, it could be an indication that the current switching is not happening as rapidly in the argon shots as it is with krypton, and that a substantial fraction of the current is still flowing in the argon even after the wire begins taking current. This would explain why even well timed argon-on-wire shots, with high voltage at the time of switching, have failed to produce radiation on the same order as the single wire controls which have much lower current at the time of breakdown.

CHAPTER 3

CONCLUSIONS

We have demonstrated the ability to transfer current from a low density imploding gas-puff shell to an axial metal wire on the 1 MA COBRA generator. The timing of this current switch is dependent upon the quantity of gas injected by the gas-puff valve, and may be controlled by adjusting the outer plenum backing pressure. We establish the time of this current transfer by noting inductive current notches in the Rogowski coil current monitor signal, and by observing the onset of thermal emission from the region of the wire, before the gas-puff pinch. X-ray pinhole images show hotspots evident of the $m=0$ instabilities seen in single-wire explosions, demonstrating substantial current flow in the wire.

Our experiments give every indication that an outer shell gas-puff implosion may function as a plasma opening switch, and we see strong evidence that this switching behavior can be used to increase x-ray yields from a central load. Si-diode and PCD measurements have shown that the timing of this switch with respect to the current pulse greatly influences the magnitude of the x-ray burst produced by the breakdown of the axial wire. With the presence of an outer shell gas-puff, x-ray yields are maximized when transfer of current to the wire occurs at or near a time of maximum dI/dt , and therefore maximum voltage. We find that for our 70 mm diameter valve on COBRA, this corresponds to an outer plenum argon backing pressure near 0.5 psi, and a krypton backing pressure of 0.35-0.4 psi. With a properly matched current pulse and gas backing pressure, we find that the Kr-on-wire configuration has the capability of producing x-ray bursts of magnitudes which significantly exceed those measured

in single-wire explosion control shots for energies above 7 keV . However the x-ray output is inconsistent in the present configuration, and is highly sensitive to gas quantity and current pulse shape.

Despite this, the measured gains in hard x-ray output measured by Si-diodes are significant, and warrant further investigation, with x-ray spectroscopy in particular, to measure how the presence of the puff affects K-shell line radiation from the wire. More experimentation is also required to fully establish what is responsible for the observed differences in functionality for different gas species, which do not seem to be solely correlated with either shell mass or particle number. Finally, additional means of optimization also merit testing, such as exploring lower backing pressures for short pulse operation, and experimenting with higher density gases such as xenon, which may offer further advantages given what's been observed with krypton.

BIBLIOGRAPHY

- [1] url: <http://plasma-gate.weizmann.ac.il/projects/experiments/plasma-opening-switches/>. Accessed 03-May-2016.
- [2] P. W.L. de Grouchy, E. Rosenberg, N. Qi, B. R. Kusse, E. Kroupp, A. Fisher, Y. Maron, and D. A. Hammer. Characterization of the cobra triple-nozzle gas-puff valve using planar laser induced fluorescence. *AIP Conference Proceedings*, 1639(1):43–46, 2014.
- [3] J. L. Giuliani and R. J. Commisso. A review of the gas-puff z -pinch as an x-ray and neutron source. *IEEE Transactions on Plasma Science*, 43(8):2385–2453, Aug 2015.
- [4] M G Haines. A review of the dense z -pinch. *Plasma Physics and Controlled Fusion*, 53(9):093001, 2011.
- [5] C. A. Jennings, D. J. Ampleford, D. C. Lamppa, S. B. Hansen, B. Jones, A. J. Harvey-Thompson, M. Jobe, T. Strizic, J. Reneker, G. A. Rochau, and M. E. Cuneo. Computational modeling of krypton gas puffs with tailored mass density profiles on za). *Physics of Plasmas*, 22(5), 2015.
- [6] B. Jones, C. A. Jennings, D. C. Lamppa, S. B. Hansen, A. J. Harvey-Thompson, D. J. Ampleford, M. E. Cuneo, T. Strizic, D. Johnson, M. C. Jones, N. W. Moore, T. M. Flanagan, J. L. McKenney, E. M. Waisman, C. A. Coverdale, M. Krishnan, P. L. Coleman, K. W. Elliott, R. E. Madden, J. Thompson, A. Bixler, J. W. Thornhill, J. L. Giuliani, Y. K. Chong, A. L. Velikovich, A. Dasgupta, and J. P. Apruzese. A renewed capability for gas puff science on sandia’s z machine. *IEEE Transactions on Plasma Science*, 42(5):1145–1152, May 2014.
- [7] J. M. Neri, J. R. Boller, P. F. Ottinger, B. V. Weber, and F. C. Young. Highvoltage, highpower operation of the plasma erosion opening switch. *Applied Physics Letters*, 50(19):1331–1333, 1987.
- [8] N. Qi, E. W. Rosenberg, P. A. Gourdain, P. W. L. de Grouchy, B. R. Kusse, D. A. Hammer, K. S. Bell, T. A. Shelkovenko, W. M. Potter, L. Atoyán, A. D. Cahill, M. Evans, J. B. Greenly, C. L. Hoyt, S. A. Pikuz, P. C. Schrafel, E. Kroupp, A. Fisher, and Y. Maron. Study of gas-puff z-pinchés on cobra. *Physics of Plasmas*, 21(11), 2014.

- [9] K. H. Schoenbach, M. Kristiansen, and G. Schaefer. A review of opening switch technology for inductive energy storage. *IEEE Proceedings*, 72:1019–1040, August 1984.
- [10] R. B. Spielman, C. Deeney, D. L. Fehl, D. L. Hanson, N. R. Keltner, J. S. McGurn, and J. L. McKenney. Fast resistive bolometry. *Review of Scientific Instruments*, 70(1):651–655, 1999.
- [11] F. J. Wessel, P. L. Coleman, N. Loter, P. Ney, H. U. Rahman, J. Rauch, and J. Thompson. Enhanced plasma radiation source: Tandem-puff, pinch-on-wire plasma. *Journal of Applied Physics*, 81(8):3410–3415, 1997.